PROMPT EMISSION OF FAST NUCLEONS IN HEAVY ION COLLISIONS*

By H. S. Köhler**

University of Arizona, Tucson and Institute for Nuclear Research, Warsaw

(Received August 24, 1981)

The prompt emission of fast nucleons resulting from the Fermi motion of nucleons in nuclei is investigated in Time-Dependent Hartree-Fock theory. The identification and demonstration of the fast nucleons (Fermi jet) is facilitated by plotting the Wigner function in phase-space. The calculations are made in one-dimensional slab-geometry. The number of nucleons in the jet varies with beam energy and with the target-projectile asymmetry. A larger asymmetry (smaller projectile) gives more nucleons. A beam of $E_{lab}/A = 24$ MeV gives a maximum number.

PACS numbers: 21.60.Jz, 24.10.-i

1. Introduction

As a consequence of the Fermi statistics a nucleon inside a cold nucleus carries an energy of kinetic motion as large as 34.5 MeV ($k_F = 1.29$ fm^{-1}). A nucleon of this energy can normally not escape from the nucleus because of the nucleon attraction. The separation energy of such a nucleon is about 8 MeV. In a collision between two nuclei the retaining potential wall disappears (or is lowered) at the point of contact between the nuclei. Nucleons are then able to flow from one nucleus over into the other [1]. Because of the relative motion between the ions some of these nucleons have velocities that are larger than the Fermi-velocity. This is illustrated by Fig. 1, which shows that, in the lab system, the velocity of the fastest nucleons is in fact equal to the sum of the Fermi-velocity v_F and the velocity V_i of the incident nucleus. This picture of the collision assumes a long mean free path. The nucleons move in a mean (self consistent) field and there are no two-body collisions, i.e., no 2p-2h excitations. This is for example consistent with the Time-Dependent Hartree-Fock (TDHF) approximation.

---

* Supported in part by U.S. National Science Foundation Grant no PHY-7902654 and Polish-U.S. Maria Skłodowska-Curie Fund under Grant P-F7F037P.

** Permanent address: Physics Department, University of Arizona, Tucson, Arizona 85721, USA.

Referring to Fig. 1, nucleons with the velocity $V_i + v_F$ that arrive at the right side of the target may have sufficient energy to escape from the system. The threshold for this to occur would be a beam energy of 0.4 MeV/nucleon, if the values of the kinetic energy and binding are those given above. If the beam energy is increased the energy of the escaping nucleons would increase rapidly as a consequence of the Fermi-motion. For a beam-energy

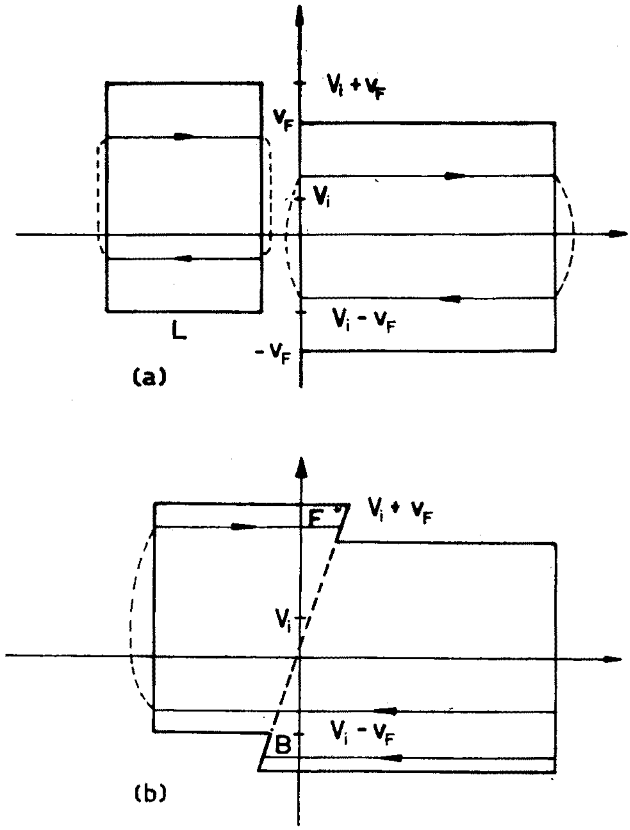

Fig. 1. A contour plot of the Wigner-function for a heavy ion-collision. The picture is qualitative only. Before the collision (a) the target occupies coordinate-space in the positive half-plane and velocity space from $-v_F$ to $+v_F$. The projectile occupies coordinate-space in the negative half space and velocity-space from $V_i - v_F$ to $V_i + v_F$, where V_i is the (collective) velocity of the projectile. The lines with arrows show nucleon trajectories with reflections at the nuclear walls (dotted lines). After the collision (b) the potential wall separating the nuclei has disappeared. Nucleons flow freely from one nucleus to the other forwards (F) and backwards (B). The F-nucleons can emerge as a fermi jet (or PEP's). The B-nucleons, coming from the larger nucleus will in general not form a jet but will scatter back. This is explained in the text

of 20 MeV/nucleon, for instance, one should see nucleons with as much energy as 65 MeV escaping. This "Fermi-jet" of nucleons or "PEP's" (Promptly Emitted Particles) should therefore, in principle be identifiable as high-energy nucleons in a heavy ion collision [2].

There are at least two factors that were omitted in the simple discussion above, each of which may be important and actually could prevent or apprecia blydecrease the occurrence of a Fermi-jet. The first of these is the attraction between the escaping nucleons both among each other as well as with the rest of the system. In a mean field theory (like TDHF) this interaction is described by a one-body potential, which is a function of the density matrix and therefore will time-evolve. As a consequence of this the potential wall on the right hand side in Fig. 1 will not be stationary in the lab system but will move with the penetrating nucleons. These nucleons may therefore be reflected back into the system even though they penetrated past the original wall. We may say that this is an effect of nuclear cohesion. As a consequence of this the number of nucleons in the Fermi-jet would be reduced. This effect is conveniently treated by calculating the time-evolvement of the nuclear self-consistent field, i.e. by a TDHF-calculation. It is found to be important.

The second factor we like to mention goes beyond the mean-field theory (e.g., TDHF) which includes only one-body dissipation, but neglects two-body collisions, i.e., 2p-2h excitations. As a consequence, the mean free path in the bulk is infinite. This agrees with the concept of the shell-model. The quasiparticle in a cold nucleus has a long mean free path; a consequence primarily of the Pauli principle. This concept survives at higher energy, e.g. in the form of the optical model or in the observation of single particle shell-model excited states. But these non-ground-state descriptions also carry with them a finite lifetime or width. For the problem at hand (the Fermi-jet) the effect of this may be included by an absorptive mean field potential [2]. In TDHF part of this absorption is included by the one-body dissipation, i.e., single-particle coupling to the surface modes. Another part, 2p-2h excitations are not included in TDHF. There is as yet not much known about the bulk mean-free path. The total absorption is obtainable from experiment but the distinction between bulk and surface absorption is more uncertain. It is believed however, that the mean free path in the bulk is essentially infinite (so that TDHF applies) for energies $E_{lab}/A \leqslant 20$ MeV. At very high energies $E_{lab}/A \geqslant 100$ MeV it is expected that hydrodynamics will apply. In the intermediate energy range a collision term has been included by the time--relaxation method [3]. The partial thermalization of the nucleons due to the two-body collisions is explicitly included by this method. In the case of a short relaxation time (short mean-free path) this thermalization may lead to hot-spots [4]. These would eject thermal nucleons which would however be less energetic than those in the Fermi-jet.

From the standpoint of gaining information on the transparency of nuclei as seen by the impinging nucleons in a heavy ion collision both the experimental and the theoretical investigation of the occurrence of Fermi-jets is important.

To pursue this, a study of the problem is presented here by performing TDHF-calculations for collisions between one-dimensional nuclear slabs. In a theoretical calculation (as in an experiment) the Fermi-jet would be characterized by nucleons that escape from the reaction-region with an energy which would be higher than that of the incident projectile. The jet would start to emerge from the interacting system just after the nucleons from the projectile have flowed through and reached the wall opposite the point of initial contact with the target nucleus.

In order to clearly identify the Fermi-jet it is therefore very convenient to display the results of calculations by contour plots of the Wigner-function, as this shows the distribution in phase-space.

Some preliminary results of this work were presented at the TDHF International Workshop at Saclay in 1979 [5]. Extensive studies of this problem in a Fermi-gas model have been made by Bondorf and coworkers [2]. Three-dimensional TDHF-calculations for ^{16}O on ^{93}Nb at $E_{lab} = 204$ MeV ($E_{lab}/A = 12.75$ MeV) have recently been reported [6]. Results are compared with the gas-model and with experiments [7]. Calculations at higher energies $E_{lab}/A = 30$ to 85 MeV of ^{12}C on ^{197}Au also support the idea of a Fermi-jet [8].

Although the 3-dimensional TDHF-calculations are decisively more realistic and informative than the one-dimensional calculations that were reported earlier [5], the latter are technically much simpler to perform. The one-dimensional space can be taken to be quite large (140 fm) so that scatterings from the walls are avoided. A large region of energies and slab sizes can be covered. Because of an apparent renewed interest in the Fermi-jet idea it was decided to present a more comprehensive report on the one-dimensional calculations. It is beleived they can provide an interesting complement to the more realistic ones. Sect. 2 briefly describes some details of the by now well-known TDHF-calculations. In Sect. 3 the results are given and conclusions are given in Sect. 4.

2. *Calculating methods*

The nucleon-nucleon effective interaction that we use is the same as in Refs. [3] and [4]. It is a local interaction (independent of relative momentum) with a $\varrho^{1/3}$-repulsion and it reproduces saturation and surface properties at standard values.

The TDHF-calculation proceeds in the one-dimensional slab-geometry mainly as in Ref. [9], a difference being the two-body force and the calculation of the Wigner-function [1]. The width of the one-dimensional box is taken to be 140 fm with a mesh size of 0.2 fm. This large box is found to be necessary in order to clearly identify nucleons as being in a Fermi jet. It exceeds the possible size in a 3-dimensional calculation. The beam energy is varied between $E_{lab}/A = 12$ MeV and $E_{lab}/A = 42$ MeV.

Preliminary calculations showed [5] that a favorable situation for a Fermi jet to emerge is an *asymmetric* collision. In addition to a low-density flow of free nucleons larger fragments (one or two) are then also seen to escape. The larger slab (target) was chosen to be 2.3 nucleons/fm^2 and the smaller slab (projectile) is chosen to be either 0.8 or 0.3 nucleons/fm^2.

3. *Results*

Fig. 2 shows a typical result displayed in phase-space by contour plots of the Wigner function at a few chosen time-steps. This result is for a slab of 0.3 nucleons/fm^2 colliding with a slab of 2.3 nucleons/fm^2 at $E_{lab}/A = 18$ MeV.

At time $t = 0$ the two slabs are separated. Two distinct plots are seen for the large and the small slab respectively. These correspond to zero temperature nuclei. The nucleons of each nucleus are constrained by the potential walls. The larger slab is moving to the left with a momentum of 0.25 fm^{-1} and the smaller to the right with 0.68 fm^{-1}.

As the nuclei collide the restraining wall between them is lowered and nucleons are free to flow across this boundary. At time $t = 0.14 \cdot 10^{-21}$ s nucleons from the smaller slab are seen to penetrate into the available domain of phase-space not already occupied by the larger slab. Nucleons from the larger slab are likewise penetrating into the smaller slab. Each slab is therefore seen to elongate in coordinate space.

At a later time, $t = 0.26 \cdot 10^{-21}$ s nucleons that can be identified as originating from the smaller slab have reached the far (right) end of the large slab. These are the nucleons

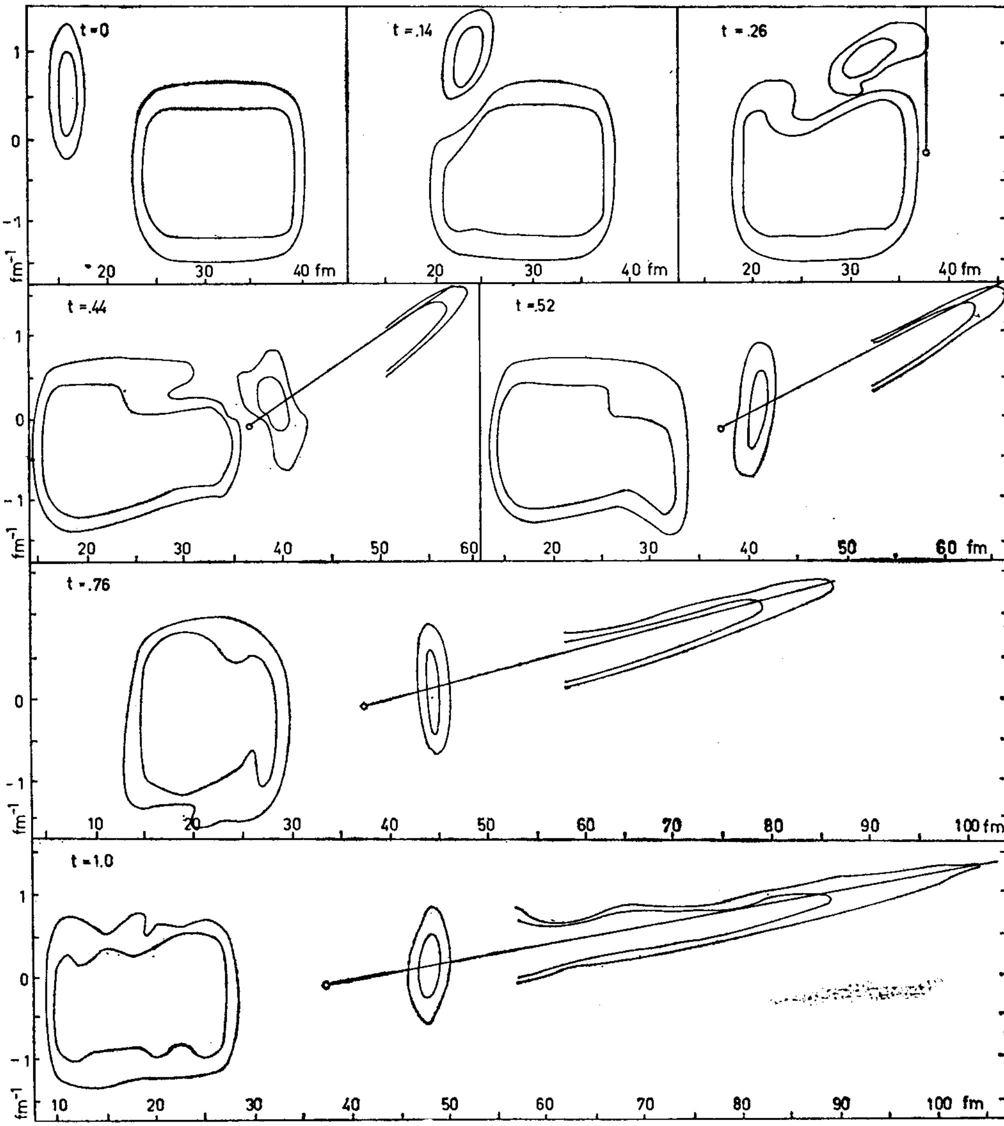

Fig. 2. Phase-space (Wigner) plots of a heavy ion collision calculated by TDHF. The collision is between two one-dimensional slabs of 0.3 and 2.3 nucleons/fm^2 respectively. Note the free nucleons escaping as a Fermi-jet and the smaller fragment of bound nucleons. The density in the jet is multiplied by a factor of 100. The time t is given in units of 10^{-21} s

that emerge as a Fermi-jet. The fastest of them (see also Fig. 3) are seen to move with a momentum, relative to the potential-wall of the larger slab, of about 1.7 fm^{-1}. Some of them will be reflected back into the system. Some nucleons that escape will move as free nucleons with a velocity that we label $\boldsymbol{v}$. They can be identified as being free nucleons by their subsequent space-coordinate $\boldsymbol{x}$ with

$$\boldsymbol{x} = \boldsymbol{v}(t-t_0), \tag{3.1}$$

where t_0 is the time of the penetration of the wall. In our case $t_0 = 0.26 \cdot 10^{-21}$ s. Equation (3.1) provides a simple identification of the Fermi-jet in the phase-space. At time t_0 a horizontal line is drawn at the edge of the nucleus from the point $k = 0$, indicated by a circle.

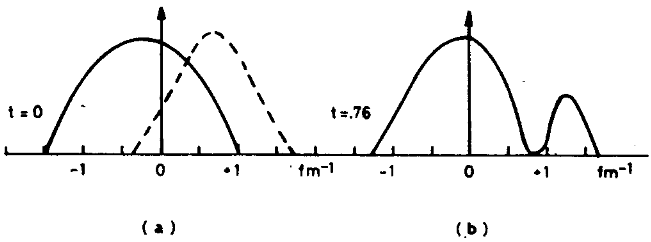

Fig. 3. The full line in (a) shows the distribution of momenta along the x-axis at $x = 34.8$ fm at $t = 0$. This is a point a few fermis inside the surface of the target. See Fig. 2. The broken line shows the distribution at 15.8 fm, i.e. inside the projectile, also at $t = 0$. In (b) the distribution at $x = 34.8$ fm is shown for $t = 26 \cdot 10^{-21}$ s. The tail of fast nucleons from the projectile has at this time arrived at this point. Compare Fig. 1 (b) and Fig. 2 at $t = 0.26 \cdot 10^{-21}$ s

At a later time any free nucleons that have escaped at $t = t_0$ would therefore be found along the line defined by Eq. (3.1) in phase-space. This line is shown in the phase-space plots for $t > t_0$. A cloud of points (nucleons) are indeed seen to follow this line as it turns with time. These nucleons are therefore free. Their momenta are in the lab system seen to be as high as 1.8 fm^{-1} (energy = 67 MeV); i.e. as predicted by the simple arguments in the Introduction. They originate from the tail of the Fermi-distribution of the projectile as detailed in Fig. 3.

There is in addition to the free nucleons also a fragment of *bound* nucleons seen in Fig. 2 with a mean momentum in lab system of $\sim$0.7 fm^{-1}. This also lies on the Fermi-jet line. Note that these nucleons can be positively identified as bound because they do not elongate in phase-space like the free nucleons. In this cloud of nucleons scatterings are taking place at the selfconsistent potential walls which prevent this elongation. In Fig. 4, to be discussed below, the bound fragment is also clearly distinguishable from the jet.

At the end of Section 2 it was stated as an empirical finding in the calculations that a Fermi-jet only emerges for asymmetric collisions [5]. This can be understood from these phase-space plots. The nucleons that start to escape at $t = t_0$ are of low density. They form a narrow distribution in momentum space when they approach the edge of the larger slab. This is because of the elongation of the distribution in phase-space discussed in relation to Fig. 2, and they consist (the fastest nucleons) of the Fermi distribution of the small slab. This is shown by the plots of momentum distributions in Fig. 3. The contribution to the selfconsistent potential of these nucleons at the edge of the larger slab is relatively small, because of their low density. (With a non-local two-body interaction this contribution would be small also because of the large momenta of these particles. See Section 4.) The opposite is the case for those nucleons of the larger slab arriving at the (left) wall of the smaller slab. These constitute the *main* contribution to the selfconsistent potential. They self-bind and do not escape but scatter back into the system.

The time-evolvement of the density distribution is shown in Fig. 4 for $E_{lab}/A = 18$ MeV and a projectile of 0.3 nucleons/fm². In this case *one* fragment (at higher beam energy *two* fragments) emerges in a deep inelastic scattering. At the tail of the distribution the density is multiplied by a factor of 200. At $t = 0.52 \cdot 10^{-21}$ s the Fermi-jet is not distin-

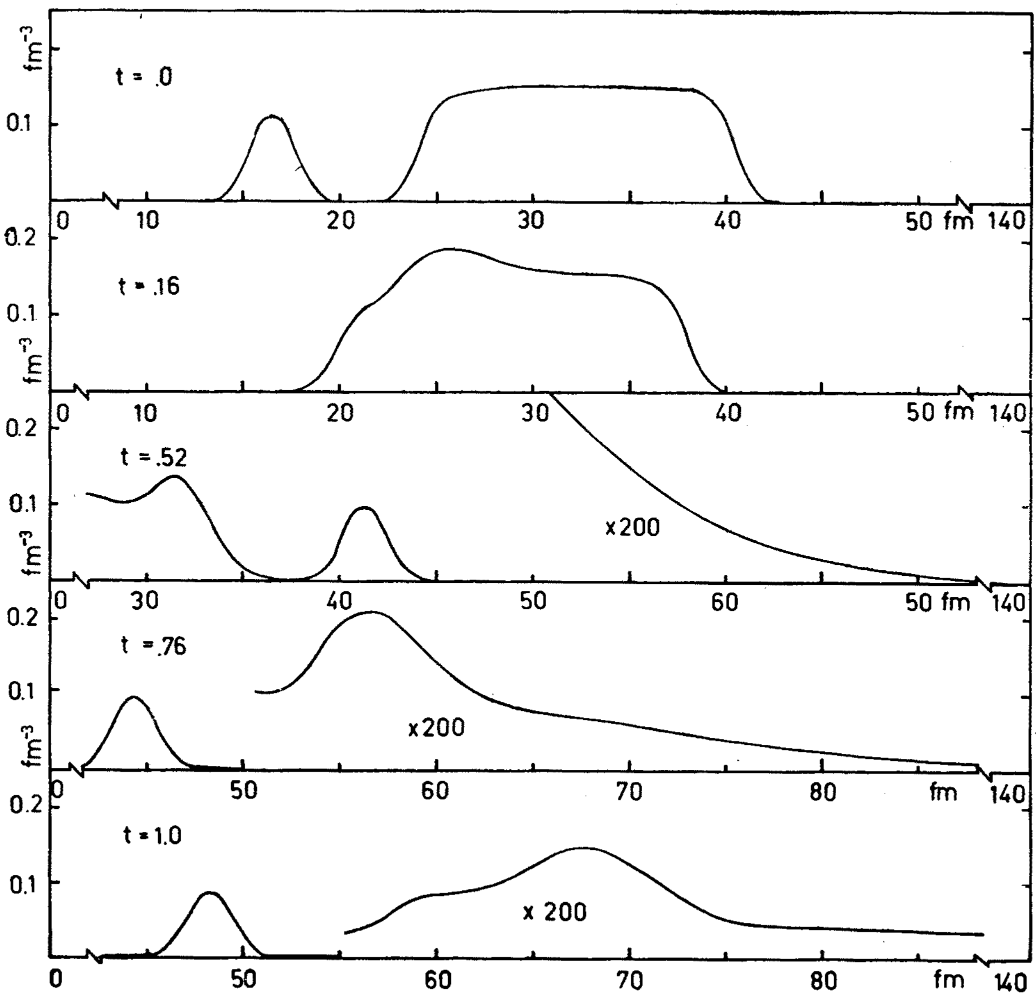

Fig. 4. Density distribution as a function of time t (in units of 10^{-21} s) obtained in TDHF. Note the multiplication by a factor of 200 in the low-density region of the jet

guishable from the fragment, while at $t = .76 \cdot 10^{-21}$ s a clear separation is seen. The free nucleons are in these plots characterised by a decrease of density with time which is caused by the dispersion of their velocities. The density of the fragment on the other hand varies only slightly because of internal collective excitation. It is however much easier to distinguish the free from the bound nucleons in the phase-space plots in Fig. 2.

Table I gives a summary of results. The number of nucleons/fm^2 of free nucleons in the jet as well as the number in the fragments is given. The jet is seen to have a maximum

TABLE I

Number of nucleons/fm^2 in the Fermi-jet of free nucleons (col. 3) and in the first and second fragments (col. 4 and 5). The second column shows the projectile energy in lab system. Upper half is for 0.3 nucleons/fm^2 in the projectile, lower half for 0.8 nucleons/fm^2. Target is 2.3 nucleons/fm^2

	MeV	Jet	1^{st} fragm.	2^{nd} fragm.
	12	.0097	.296	.0
	18	.0137	.262	.0
0.3 → 2.3	24	.0151	.192	.083
	30	.0105	.128	.152
	36	.0089	.121	.153
	18	.0019	.326	.0
	24	.0022	.280	.266
0.8 → 2.3	30	.0021	.262	.256
	36	.0018	.258	.256
	42	.0018	.257	.218

at $E_{lab}/A = 24$ MeV while the first (fastest) fragment is seen to decrease with beam-energy. The slower, second fragment is seen to increase in size in case of the small projectile but decrease (although rather slowly) in case of the larger projectile.

4. *Conclusions*

Our calculations show that a Fermi-jet of fast and free nucleons is seen to emerge in a heavy-ion collision in the TDHF-approximation. The result is in general agreement with the simple mechanism described in Sect. 1, (Fig. 1), in which the Fermi motion of the nucleons is added to the momentum of the incident nucleus. This mechanism has been implicated by Bondorf et al. [2] in semi-classical calculations.

It is somewhat ambiguous to translate the results of our one-dimensional slab calculations to an expectation for real nuclei. We should however be able to at least obtain an order of magnitude estimate for head-on collisions between real nuclei. To this end we assume that the impact area or window for the collision is 10 fm^2. (This would actually be the approximate area of the smallest slab). With this assumption we find a maximum of ~0.15 nucleons in the jet for the 0.3 slab at 24 MeV. This is followed by a fragment of approximately the size of an α-particle.

The three-dimensional calculation of Devi et al. [6] with an ^{16}O beam at $E_{lab}/A = 12.75$ MeV on ^{93}Nb gives a Fermi-jet of 0.6 nucleons per event for head-on collisions (and a decrease with impact parameter). There is no immediate explanation for the factor of 4 difference.

It has to be pointed out however that a positive identification of the Fermi-jet and a determination of momenta is made in the present calculation. This is made possible not only because of the simpler geometry but also by the plots of the Wigner-function. The use of a large space (140 fm) to accomodate the fast nucleons and prevent back-scatterings from the walls is also important. As seen in Fig. 4, a clean separation of the jet does not occur until $t \sim 10^{-21}$ s or until about $\sim 0.5 \cdot 10^{-21}$ s after it first emerges and it then occupies a minimum of 20 fm of length. In the case of the heavier projectile 0.8 nucleons/fm^2 the situation is somewhat more favorable as the time lapse until separation is only $\sim 10^{-22}$ s. This appears to be the situation in the calculations of Devi et al. [6].

A local two-body force was used in the present calculations. This force enters in the calculations in the generation of the mean field (Hartree-Fock) potential which then also will be local. As a consequence all nucleons, independent of their momentum, will move in a potential of the same depth. In the case of a non-local interaction the fast nucleons would move in a shallower potential and would therefore escape easier. Devi et al. [6] use a non-local interaction in their calculations. This might explain the apparently larger Fermi-jet observed by them.

I wish to thank Professor Janusz Dąbrowski for the hospitality at the Nuclear Theory Department of the Institute for Nuclear Research in Warsaw where this work was completed.

REFERENCES

[1] H. S. Köhler, H. Flocard, *Nucl. Phys.* **A323**, 189 (1979).
[2] J. P. Bondorf, J. N. De, G. Fái, A. O. T. Karvinen, B. Jakobsson, J. Randrup, *Nucl. Phys.* **A333**, 285 (1980); J. P. Bondorf, J. N. De, G. Fái, A. O. T. Karvinen, B. Jakobsson, *Phys. Lett.* **84B**, 163 (1979).
[3] H. S. Köhler, *Nucl. Phys.* **A343**, 315 (1980).
[4] H. S. Köhler, submitted to *Nuclear Physics* for publication.
[5] H. S. Köhler, in *Time Dependent Hartree-Fock Methods*, ed. P. Bonche, B. Giraud, P. Quentin, May 1979, p. 1.
[6] K. R. S. Devi, M. R. Strayer, K. T. R. Davies, S. E. Koonin, A. K. Dhar, preprint June 1981.
[7] A. Gavron, R. L. Ferguson, F. E. Obenshain, F. Plasil, G. R. Young, G. A. Pettit, K. A. Geoffroy, D. G. Sarantites, C. F. Maguire, unpublished (1981).
[8] H. Stöcker, R. Y. Cusson, J. A. Maruhn, W. Greiner, *Phys. Lett.* **101B**, 379 (1981).
[9] P. Bonche, S. Koonin, T. W. Negele, *Phys. Rev.* **C13**, 1226 (1976).